COURANT NUMBER INSENSITIVE CE/SE SCHEMES

Sin-Chung Chang*
NASA Glenn Research Center, Cleveland, OH 44135

Abstract

The stability of a CE/SE scheme requires that the *CFL* number < 1. Without using special techniques that involve ad hoc parameters, generally the numerical dissipation associated with a CE/SE simulation with a fixed total marching time increases as the *CFL* number decreases. As a result, for a small *CFL* number (say < 0.1), a CE/SE scheme may become overly dissipative. In this paper, using Sod's shock tube problem as an example, it is demonstrated that a parameter-free CE/SE scheme constructed here can resolve shocks and contact discontinuities crisply for the *CFL* number ranging from close to 1 to less than 0.001.

1. Introduction

The space-time conservation element and solution element (CE/SE) method is a high-resolution and genuinely multidimensional method for solving conservation laws [1–35]. The CE/SE method differs substantially in both concept and methodology from the well-established methods. Its nontraditional features include a unified treatment of space and time, the introduction of space-time staggered conservation elements and solution elements, a novel shock-capturing strategy that does not use Riemann solvers, and above all, a mathematically simple and yet physics-solid logical structure that accounts for the method's simplicity, robustness and accuracy. Note that conservation elements are nonoverlapping space-time subdomains introduced such that (i) the computational domain is the union of these subdomains; and (ii) flux conservation can be enforced over each of them and also over the union of any combination of them. On the other hand, each solution element is a space-time subdomain over which any physical flux vector is approximated using simple smooth functions. In general, a conservation element does not coincide with a solution element.

To date, numerous highly accurate CE/SE steady and unsteady solutions with Mach numbers ranging from 0.0028 to 10 have been obtained without using preconditioning or other special techniques [28]. The flow phenomena modeled include traveling and interacting shocks, acoustic waves, shedding vortices, detonation waves, cavitation, and hydraulic jump [1–35]. In particular, the rather unique capability of the CE/SE method to resolve both strong shocks and small disturbances (e.g., acoustic waves) simultaneously has been verified through several accurate predictions of experimental data [13,14]. Note that, *while numerical dissipation is required for shock resolution, it may also result in annihilation of small disturbances. Thus a solver that can handle both strong shocks and small disturbances simultaneously must be able to overcome this difficulty.*

In spite of its past successes, there is still room for improving the CE/SE method. An example is the fact that, for a practical CE/SE simulation with a fixed total marching time, local numerical dissipation tends to increase as local *CFL* number decreases. As a result, without using special techniques (see Sec. 2) that involve ad hoc parameters, a CE/SE solution may become overly dissipative at some region if its local *CFL* number becomes too small (say < 0.1). In a numerical simulation involving a highly nonuniform spatial mesh and a spatially independent time step, the values of local *CFL* number may vary sharply across the computational domain. As a result, these values may range from its maximum stability bound, i.e., 1, to a value $\ll 1$. For this case, the performance sensitivity of a CE/SE scheme with respect to the variation of the local *Courant* number obviously can result in a solution that is highly dissipative in a regions where the local *CFL* number $\ll 1$.

In this paper we shall describe how one can construct parameter-free and Courant-number insensitive CE/SE schemes. The rest of the paper is organized as follows. A review of the existing CE/SE schemes is given in Sec. 2. The new Courant-number insensitive schemes are described in Sec. 3. Using Sod's shock tube problem [36] as an example, it is shown in Sec. 4 that the Euler version of a new scheme described in Sec. 3 can resolve shocks and contact discontinuities crisply for the *CFL* number ranging from 1 to 0.001. Concluding remarks are

*Aerospace Engineer, Member AIAA
email: sin-chung.chang@grc.nasa.gov
This paper is declared a work of the U.S. Government and is not subject to copyright protection in the United States.

given in Sec. 5. Finally, to give the reader a concrete idea about the simplicity and robustness of the CE/SE method in general and the new schemes in particular, the short Fortran program used to generate the present numerical results is listed in Appendix.

2. Review of the 1D CE/SE method

For simplicity, we review the existing CE/SE schemes for the PDE

$$\frac{\partial u}{\partial t} + a\frac{\partial u}{\partial x} = 0 \tag{2.1}$$

where $a \neq 0$ is a constant. Let $x_1 = x$, and $x_2 = t$ be considered as the coordinates of a two-dimensional Euclidean space E_2. Then, by using Gauss' divergence theorem in the space-time E_2, it can be shown that Eq. (2.1) is the differential form of the integral conservation law

$$\oint_{S(V)} \vec{h} \cdot d\vec{s} = 0 \tag{2.2}$$

As depicted in Fig. 1, here (i) $S(V)$ is the boundary of an arbitrary *space-time* region V in E_2, (ii) $\vec{h} = (au, u)$, and (iii) $d\vec{s} = d\sigma\,\vec{n}$ with $d\sigma$ and $\vec{n}$, respectively, being the area and the unit outward normal of a surface element on $S(V)$. Note that: (i) because $\vec{h} \cdot d\vec{s}$ is the *space-time* flux of $\vec{h}$ leaving the region V through the surface element $d\vec{s}$, Eq. (2.2) simply states that the total *space-time* flux of $\vec{h}$ leaving V through $S(V)$ vanishes; (ii) in E_2, $d\sigma$ is the length of a line segment on the simple closed curve $S(V)$; and (iii) all mathematical operations can be carried out as though E_2 were an ordinary two-dimensional Euclidean space.

To proceed, let Ω denote the set of all space-time staggered mesh points in E_2 (dots in Fig. 2(a)), where $n = 0, \pm 1/2, \pm 1, \pm 3/2, \pm 2, \ldots$, and, for each n, $j = n \pm 1/2, n \pm 3/2, n \pm 5/2, \ldots$. Each $(j,n) \in \Omega$ is associated with a solution element, i.e., SE(j,n). By definition, SE(j,n) is the *interior* of the *space-time* region bounded by a dashed curve depicted in Fig. 2(b). It includes a horizontal line segment, a vertical line segment, and their immediate neighborhood.

Let $(x,t) \in$ SE(j,n). Then Eq. (2.2) will be simulated numerically assuming that $u(x,t)$ and $\vec{h}(x,t)$, respectively, are approximated by

$$u^*(x,t\,;j,n) \stackrel{\text{def}}{=} u_j^n + (u_x)_j^n (x - x_j) + (u_t)_j^n (t - t^n) \tag{2.3}$$

and

$$\vec{h}^*(x,t\,;j,n) \stackrel{\text{def}}{=} \big(au^*(x,t\,;j,n),\, u^*(x,t\,;j,n)\big) \tag{2.4}$$

Note that (i) u_j^n, $(u_x)_j^n$, and $(u_t)_j^n$ are constants in SE(j,n), (ii) (x_j, t^n) are the coordinates of the mesh point (j,n) with $x_j = j\Delta x$ and $t^n = n\Delta t$, and (iii) Eq. (2.4) is the numerical analogue of the definition $\vec{h} = (au, u)$.

Let $u = u^*(x,t\,;j,n)$ satisfy Eq. (2.1) within SE(j,n). Then one has $(u_t)_j^n = -a\,(u_x)_j^n$. As a result, Eq. (2.3) reduces to

$$u^*(x,t\,;j,n) = u_j^n + (u_x)_j^n \left[(x - x_j) - a\,(t - t^n)\right], \tag{2.5}$$

for $(x,t) \in$ SE(j,n), i.e., u_j^n and $(u_x)_j^n$ are the only independent marching variables associated with (j,n).

Let E_2 be divided into nonoverlapping rectangular regions (see Fig. 2(a)). As depicted in Figs. 2(c)–2(e), (i) two such regions, i.e., CE$_-(j,n)$ and CE$_+(j,n)$, are associated with each interior mesh point $(j,n) \in \Omega$; and (ii) CE(j,n) is the union of CE$_-(j,n)$ and CE$_+(j,n)$.

Given the above preliminaries, we are ready to describe the existing CE/SE solvers for Eq. (2.1).

2.1. The a Scheme

Note that, among the line segments forming the boundary of CE$_-(j,n)$, $\overline{AB}$ and $\overline{AD}$ belong to SE(j,n), while $\overline{CB}$ and $\overline{CD}$ belong to SE$(j-1/2, n-1/2)$. Similarly, the boundary of CE$_+(j,n)$ belongs to either SE(j,n) or SE$(j+1/2, n-1/2)$. As a result, by imposing two conservation conditions at each $(j,n) \in \Omega$, i.e.,

$$\oint_{S(CE_+(j,n))} \vec{h}^* \cdot d\vec{s} = 0, \quad \text{and}$$

$$\oint_{S(CE_-(j,n))} \vec{h}^* \cdot d\vec{s} = 0, \qquad (j,n) \in \Omega \tag{2.6}$$

and using Eqs. (2.4) and (2.5), one can obtain two equations for the two unknowns u_j^n and $(u_x)_j^n$. By solving these equations, one has (i)

$$u_j^n = \frac{1}{2}\Big\{(1+\nu)u_{j-1/2}^{n-1/2} + (1-\nu)u_{j+1/2}^{n-1/2} + (1-\nu^2)\left[(u_x^+)_{j-1/2}^{n-1/2} - (u_x^+)_{j+1/2}^{n-1/2}\right]\Big\} \tag{2.7}$$

and, assuming $1 - \nu^2 \neq 0$, (ii)

$$(u_x^+)_j^n = (u_x^{a+})_j^n \tag{2.8}$$

with

$$(u_x^{a+})_j^n \stackrel{\text{def}}{=} \frac{1}{2}\Big[u_{j+1/2}^{n-1/2} - u_{j-1/2}^{n-1/2} - (1-\nu)(u_x^+)_{j-1/2}^{n-1/2} - (1+\nu)(u_x^+)_{j+1/2}^{n-1/2}\Big] \tag{2.9}$$

Here, (i) $\nu \stackrel{\text{def}}{=} a\Delta t/\Delta x$, and (ii) for any $(j,n) \in \Omega$,

$$(u_x^+)_j^n \stackrel{\text{def}}{=} \frac{\Delta x}{4}(u_x)_j^n \tag{2.10}$$

The a scheme, i.e., the inviscid case of the a-μ scheme [1,3,9], is formed by Eqs. (2.7) and (2.8). Note that: (i) hereafter the superscript symbol "+" is used to denote a *normalized* parameter; and (ii) the superscript symbol "a" in the parameter $(u_x^{a+})_j^n$ is introduced to remind the reader that Eq. (2.8) is valid for the a scheme.

The review of the a scheme is concluded with the following remarks:

(a) As shown in [3], the two amplification factors of the a scheme are identical to those of the leapfrog scheme. As a result, the a scheme is nondissipative and it is stable if $\nu^2 < 1$.

(b) Note that derivation of Eqs. (2.7) and (2.8) can be facilitated by the following observations: because $u^*(x,t;j,n)$ is linear in x and t, it can be shown that the total flux of $\vec{h}^*$ leaving $\text{CE}_-(j,n)$ or $\text{CE}_+(j,n)$ through any of the four line segments that form its boundary is equal to the scalar product of the vector $\vec{h}^*$ evaluated at the midpoint of the line segment and the "surface" vector (i.e., the unit outward normal multiplied by the length) of the line segment.

(c) Because, for any $(j,n) \in \Omega$, the total flux of $\vec{h}^*$ leaving each of $\text{CE}_-(j,n)$ and $\text{CE}_+(j,n)$ vanishes (see Eq. (2.6)), *$CE_-(j,n)$ and $CE_+(j,n)$, $(j,n) \in \Omega$, will be referred to as the conservation elements (CEs) of the a scheme.* In addition, because the surface integration over any interface separating two neighboring CEs is evaluated using the information from a single SE, obviously the flux leaving one of these CEs through the interface is the negative of that leaving another CE through the same interface. As a result, the local conservation relations Eq. (2.6) lead to a global flux conservation relation, i.e., *the total flux of $\vec{h}^*$ leaving the boundary of any space-time region that is the union of any combination of CEs will also vanish.* In particular, because $\text{CE}(j,n)$ is the union of $\text{CE}_-(j,n)$ and $\text{CE}_+(j,n)$,

$$\oint_{S(CE(j,n))} \vec{h}^* \cdot d\vec{s} = 0, \quad (j,n) \in \Omega \tag{2.11}$$

must follow from Eq. (2.6). In fact, *it can be shown that Eq. (2.11) is equivalent to Eq. (2.7).*

(d) In addition to the nondissipative a scheme, as will be shown, there is a family of its dissipative extensions in which *only the less stringent conservation condition Eq. (2.11) is assumed* [3]. Because Eq. (2.11) is equivalent to Eq. (2.7), for each of these extensions, u_j^n is still evaluated using Eq. (2.7) while $(u_x^+)_j^n$ is evaluated using an equation different from Eq. (2.8).

2.2. The a-ϵ Scheme

To proceed, consider any $(j,n) \in \Omega$. Then $(j \pm 1/2, n-1/2) \in \Omega$. Let

$$u'^n_{j\pm1/2} \stackrel{\text{def}}{=} u^{n-1/2}_{j\pm1/2} + (\Delta t/2)(u_t)^{n-1/2}_{j\pm1/2} \tag{2.12}$$

Substituting Eq. (2.10) and the relation $(u_t)_j^n = -a(u_x)_j^n$ into Eq. (2.12) and using the definition $\nu = a\Delta t/\Delta x$, one has

$$u'^n_{j\pm1/2} = \left[u - 2\nu\, u_x^+\right]^{n-1/2}_{j\pm1/2} \stackrel{\text{def}}{=} u^{n-1/2}_{j\pm1/2} - 2\nu(u_x^+)^{n-1/2}_{j\pm1/2} \tag{2.13}$$

Note that, by definition, $(j\pm1/2,n) \notin \Omega$ if $(j,n) \in \Omega$. Thus $u'^n_{j\pm1/2}$ is associated with a mesh point $\notin \Omega$. The reader is warned that similar situations may occur in the rest of this paper.

According to Eq. (2.12), $u'^n_{j\pm1/2}$ can be interpreted as a first-order Taylor's approximation of u at $(j \pm 1/2, n)$. Thus

$$(u_x^{c+})_j^n \stackrel{\text{def}}{=} \frac{u'^n_{j+1/2} - u'^n_{j-1/2}}{4} = \frac{\Delta x}{4}\left(\frac{u'^n_{j+1/2} - u'^n_{j-1/2}}{\Delta x}\right) \tag{2.14}$$

is a central-difference approximation of $\partial u/\partial x$ at (j,n), normalized by the same factor $\Delta x/4$ that appears in Eq. (2.10). Note that the superscript "c" is used to remind the reader of the central-difference nature of the term $(u_x^{c+})_j^n$. The a-ϵ scheme is formed by Eq. (2.7) and

$$(u_x^+)_j^n = (u_x^{a+})_j^n + 2\epsilon(u_x^{c+} - u_x^{a+})_j^n \tag{2.15}$$

where ϵ is a real number. Obviously the a-ϵ scheme reduces to the a scheme when $\epsilon = 0$. Also, for the case $\epsilon = 1/2$, Eq. (2.15) reduces to

$$(u_x^+)_j^n = (u_x^{c+})_j^n \tag{2.16}$$

Note that the first part of the expression on the right side of Eq. (2.15), i.e., $(u_x^{a+})_j^n$, emerges from the development of the non-dissipative a scheme. As a result, it is the non-dissipative part. On the other hand, the second part, whose magnitude can be adjusted by the parameter ϵ, represents numerical dissipation introduced by the difference between the central difference term $(u_x^{c+})_j^n$ and the non-dissipative term $(u_x^{a+})_j^n$. Thus one may heuristically conclude that the numerical dissipation associated

with the a-ϵ scheme can be increased by increasing the value of ϵ. It was shown in [3] that this conclusion is indeed valid in the stability domain of the a-ϵ scheme, i.e.,

$$0 \le \epsilon \le 1, \qquad \text{and} \qquad \nu^2 < 1 \tag{2.17}$$

2.3. The a-ϵ-α-β Scheme

If discontinuities are present in a numerical solution, the a-ϵ scheme is not equipped to suppress numerical wiggles that generally appear near these discontinuities. The a-ϵ-α-β scheme was introduced as a remedy for this deficiency.

To proceed, let

$$(u_{x+}^{c+})_j^n \stackrel{\text{def}}{=} \frac{1}{2}(u'^n_{j+1/2} - u_j^n) = \frac{\Delta x}{4}\left(\frac{u'^n_{j+1/2} - u_j^n}{\Delta x/2}\right) \tag{2.18}$$

$$(u_{x-}^{c+})_j^n \stackrel{\text{def}}{=} \frac{1}{2}(u_j^n - u'^n_{j-1/2}) = \frac{\Delta x}{4}\left(\frac{u_j^n - u'^n_{j-1/2}}{\Delta x/2}\right) \tag{2.19}$$

i.e., $(u_{x+}^{c+})_j^n$ and $(u_{x-}^{c+})_j^n$ are two (normalized) numerical analogues of the value of $\partial u/\partial x$ at (j,n) with one being evaluated from the right and another from the left. It can be shown that

$$(u_x^{c+})_j^n = \frac{1}{2}\left[(u_{x+}^{c+})_j^n + (u_{x-}^{c+})_j^n\right] \tag{2.20}$$

i.e., $(u_x^{c+})_j^n$ is the simple average of $(u_{x+}^{c+})_j^n$ and $(u_{x-}^{c+})_j^n$. Next, let the function W_o be defined by (i) $W_o(0,0,\alpha) = 0$ and (ii)

$$W_o(x_-, x_+; \alpha) = \frac{|x_+|^\alpha x_- + |x_-|^\alpha x_+}{|x_+|^\alpha + |x_-|^\alpha}, \ (|x_+|+|x_-| > 0) \tag{2.21}$$

where x_+, x_- and $\alpha \ge 0$ are real variables. Note that (i) to avoid dividing by zero, in practice a small positive number such as 10^{-60} is added to the denominator in Eq. (2.21); and (ii) $W_o(x_-, x_+; \alpha)$, a nonlinear weighted average of x_- and x_+, becomes their simple average if $\alpha = 0$ or $|x_-| = |x_+|$. Furthermore, let

$$(u_x^{w+})_j^n \stackrel{\text{def}}{=} W_o\left((u_{x+}^{c+})_j^n, (u_{x-}^{c+})_j^n; \alpha\right) \tag{2.22}$$

Note that the superscript "w" is used to remind the reader of the weighted-average nature of the term $(u_x^{w+})_j^n$. With the aid of the above definitions, a more advanced scheme, referred to as the a-ϵ-α-β scheme, can be defined by Eq. (2.7) and

$$(u_x^+)_j^n = (u_x^{a+})_j^n + 2\epsilon(u_x^{c+} - u_x^{a+})_j^n + \beta(u_x^{w+} - u_x^{c+})_j^n \tag{2.23}$$

Here $\beta \ge 0$ is another adjustable constant. It can be shown that the a-ϵ-α-β scheme reduces to the a-ϵ scheme if $\alpha = 0$ or $\beta = 0$. Also, for the special case that $\epsilon = 1/2$ and $\beta = 1$, Eq. (2.23) reduces to

$$(u_x^+)_j^n = (u_x^{w+})_j^n \tag{2.24}$$

Hereafter the scheme formed by Eq. (2.7) and (2.24) will be referred to as the a-α scheme. It has been shown numerically that the a-α scheme is stable if $\nu^2 < 1$ and $\alpha \ge 0$.

The expression on the right side of Eq. (2.23) contains three parts. The first part is a non-dissipative term $(u_x^{a+})_j^n$. The second part is the product of 2ϵ and the difference between the central difference term $(u_x^{c+})_j^n$ and the non-dissipative term $(u_x^{a+})_j^n$. The third part is the product of β and the difference between a weighted average of $(u_{x+}^{c+})_j^n$ and $(u_{x-}^{c+})_j^n$ and their simple average. Numerical dissipation introduced by the second part generally is effective in damping out numerical instabilities that arise from the smooth region of a solution. But it is less effective in suppressing numerical wiggles that often occur near a discontinuity. On the other hand, numerical dissipation introduced by the third part is very effective in suppressing numerical wiggles. Moreover, because the condition $|(u_{x+}^{c+})_j^n| = |(u_{x-}^{c+})_j^n|$ more or less prevails and thus the weighted average is nearly equal to the simple average (see comment (ii) given immediately following Eq. (2.21)) in the smooth region of the the solution, numerical dissipation introduced by the third part has very slight effect in the smooth region.

From the above discussion, one concludes that there are two different types of numerical dissipation associated with the a-ϵ-α-β scheme and they complement each other. As a result, the a-ϵ-α-β scheme, in principle, is capable of handling both small disturbances and sharp discontinues simultaneously if the values of ϵ, α and β are chosen properly. Assuming that the spatial mesh used is uniform, the choice with $\epsilon = 1/2$, $\alpha = 1, 2$ and $\beta = 1$ (i.e., using Eqs. (2.7) and (2.24) with $\alpha = 1, 2$) generally will result in decent CE/SE solutions if the absolute value of ν is not too small. However, for a more challenging situation, the parameter ϵ and β generally must be considered as functions of ν such as those suggested in [3,7], i.e.,

$$\epsilon(\nu) = 0.5\,\nu\exp(1-\nu) \quad \text{and} \quad \beta(\nu) = \sqrt{\nu}, \ 0 \le \nu \le 1 \tag{2.25}$$

Even though the use of Eq. (2.25) and its Euler version was a success in some cases [3], the ad hoc nature of the approach is fundamentally not satisfying. In the following, we present a simpler and more robust approach.

3. New schemes

To proceed, note that the a-α scheme ($\alpha = 1, 2$) is very accurate as long as $0.1 < \nu^2 < 1$. However, it becomes very diffusive when $|\nu| \ll 1$. To overcome this weakness, in the following we shall construct a new scheme that reduces to (i) the a-α scheme in the limit of $|\nu| \to 1$, and (ii) the nondissipative a scheme in the limit of $\nu \to 0$. As a prerequisite, we shall first study the a scheme in the limit of $\nu \to 0$.

The a scheme is formed by Eqs. (2.7) and (2.8). It can be shown easily that, in the limit of $\nu \to 0$, these equations are equivalent to the system of equations

$$u_j^n + (u_x^+)_j^n = u_{j+1/2}^{n-1/2} - (u_x^+)_{j+1/2}^{n-1/2} \tag{3.1}$$

and

$$u_j^n - (u_x^+)_j^n = u_{j-1/2}^{n-1/2} + (u_x^+)_{j-1/2}^{n-1/2} \tag{3.2}$$

Note that, with the aid of Remark (b) given at the end of Sec. 2.1, it can be shown easily that, in the limit of $\Delta t \to 0$ with a and Δx being held constant, the two conservation conditions given in Eq.(2.6) reduce to Eqs. (3.1) and (3.2), respectively. This conclusion is consistent with the definition $\nu = a\Delta t/\Delta x$ and the fact that Eqs. (2.7) and (2.8) are equivalent to Eq. (2.6) if $1 - \nu^2 \neq 0$.

To construct the new scheme, let P_-, M_-, M_+, and P_+ be the points depicted in Fig. 3. Then, as the value of $|\nu|$ decreases from 1 to 0, point P_+ will move from the mesh point $(j + 1/2, n)$ to point M_+, the midpoint of the line segment joining the mesh points (j, n) and $(j+1/2, n)$). On the other hand, point P_- will move from the mesh point $(j - 1/2, n)$ to point M_-, the midpoint of the line segment joining the mesh points (j, n) and $(j - 1/2, n)$).

Let

$$u'(P_+) \stackrel{\text{def}}{=} u_{j+1/2}^{n-1/2} + \frac{\Delta t}{2}(u_t)_{j+1/2}^{n-1/2} - \frac{(1-|\nu|)\Delta x}{4}(u_x)_{j+1/2}^{n-1/2} \tag{3.3}$$

$$u'(P_-) \stackrel{\text{def}}{=} u_{j-1/2}^{n-1/2} + \frac{\Delta t}{2}(u_t)_{j-1/2}^{n-1/2} + \frac{(1-|\nu|)\Delta x}{4}(u_x)_{j-1/2}^{n-1/2} \tag{3.4}$$

Then $u'(P_+)$ is a first-order Taylor's approximation of u at point P_+ evaluated using the marching variables at $(j+1/2, n-1/2)$ while $u'(P_-)$ is a first-order Taylor's approximation of u at point P_- evaluated using the marching variables at $(j - 1/2, n - 1/2)$. Also note that, by using Eq. (2.10) and the relation $(u_t)_j^n = -a(u_x)_j^n$, Eqs. (3.3) and (3.4) can be simplified as

$$u'(P_+) = \left[u - (1 + 2\nu - |\nu|)\, u_x^+\right]_{j+1/2}^{n-1/2} \tag{3.5}$$

and

$$u'(P_-) = \left[u + (1 - 2\nu - |\nu|)\, u_x^+\right]_{j-1/2}^{n-1/2} \tag{3.6}$$

respectively. Thus one has (i)

$$u'(P_+) = \left[u - 2\nu u_x^+\right]_{j+1/2}^{n-1/2} \quad \text{and}$$

$$u'(P_-) = \left[u - 2\nu u_x^+\right]_{j-1/2}^{n-1/2} \quad \text{if } |\nu| = 1 \tag{3.7}$$

and (ii)

$$u'(P_+) = \left[u - u_x^+\right]_{j+1/2}^{n-1/2} \quad \text{and}$$

$$u'(P_-) = \left[u + u_x^+\right]_{j-1/2}^{n-1/2} \quad \text{if } \nu = 0 \tag{3.8}$$

To proceed, let

$$(\hat{u}_x^+)_j^n \stackrel{\text{def}}{=} \frac{u'(P_+) - u'(P_-)}{2(1+|\nu|)} = \frac{\Delta x}{4}\left(\frac{u'(P_+) - u'(P_-)}{(1+|\nu|)\Delta x/2}\right) \tag{3.9}$$

$$(\hat{u}_{x+}^+)_j^n \stackrel{\text{def}}{=} \frac{u'(P_+) - u_j^n}{1+|\nu|} = \frac{\Delta x}{4}\left(\frac{u'(P_+) - u_j^n}{(1+|\nu|)\Delta x/4}\right) \tag{3.10}$$

$$(\hat{u}_{x-}^+)_j^n \stackrel{\text{def}}{=} \frac{u_j^n - u'(P_-)}{1+|\nu|} = \frac{\Delta x}{4}\left(\frac{u_j^n - u'(P_-)}{(1+|\nu|)\Delta x/4}\right) \tag{3.11}$$

$$(\hat{u}_x^{w+})_j^n \stackrel{\text{def}}{=} W_o\left((\hat{u}_{x+}^+)_j^n, (\hat{u}_{x-}^+)_j^n; \alpha\right) \tag{3.12}$$

Because the mesh point (j, n) is the midpoint of the line segment $\overline{P_-P_+}$ and the length of $\overline{P_-P_+}$ is $(1 + |\nu|)\Delta x/2$, Eq. (3.9) implies that $(\hat{u}_x^+)_j^n$ is a central-difference approximation of the value of $\partial u/\partial x$ at (j, n), normalized by the factor $\Delta x/4$. On the other hand, Eqs. (3.10) and (3.11) imply that $(\hat{u}_{x+}^+)_j^n$ and $(\hat{u}_{x-}^+)_j^n$ are two (normalized) one-sided difference approximations of the value of $\partial u/\partial x$ at (j, n) with one being evaluated from the right and another from the left. Moreover, because

$$(\hat{u}_x^+)_j^n = \frac{1}{2}\left[(\hat{u}_{x+}^+)_j^n + (\hat{u}_{x-}^+)_j^n\right] \tag{3.13}$$

Eq. (2.21) implies that

$$(\hat{u}_x^{w+})_j^n = (\hat{u}_x^+)_j^n \quad \text{if } \alpha = 0 \text{ or } |(\hat{u}_{x+}^+)_j^n| = |(\hat{u}_{x-}^+)_j^n| \tag{3.14}$$

With the above preliminaries, a new solver for Eq. (2.1), referred to as Scheme I in this paper, is formed by Eq. (2.7) and

$$(u_x^+)_j^n = (\hat{u}_x^{w+})_j^n \tag{3.15}$$

In the following, we shall prove that Scheme I does meet the requirements set forth earlier in this section.

Consider the limiting case that $|\nu| = 1$. Eqs. (2.13) and (3.7) imply that

$$u'(P_+) = u'^n_{j+1/2} \text{ and } u'(P_-) = u'^n_{j-1/2} \quad (|\nu| = 1) \tag{3.16}$$

As a result, Eqs. (2.18), (2.19), (3.10) and (3.11) imply that

$$(\hat{u}^{+}_{x+})^n_j = (u^{c+}_{x+})^n_j \text{ and } (\hat{u}^{+}_{x-})^n_j = (u^{c+}_{x-})^n_j \quad (|\nu| = 1) \tag{3.17}$$

Combining Eqs. (2.22), (3.12) and (3.17), one concludes that

$$(\hat{u}^{w+}_{x})^n_j = (u^{w+}_{x})^n_j \qquad (|\nu| = 1) \tag{3.18}$$

Thus Scheme I (formed by Eqs. (2.7) and (3.15), reduces to the a-α scheme (formed by Eqs. (2.7) and (2.24)) in the limit of $|\nu| \to 1$.

Next consider the limiting case that $\nu = 0$. According to Eq. (3.8), for this case $u'(P_+)$ and $u'(P_-)$, respectively, reduce to the expressions on the right sides of Eqs. (3.1) and (3.2). Because $(u^{+}_{x})^n_j = (u^{a+}_{x})^n_j$ for the a scheme, one concludes that, in the case that $\nu = 0$,

$$u^n_j + (u^{a+}_{x})^n_j = u'(P_+) \qquad (\nu = 0) \tag{3.19}$$

$$u^n_j - (u^{a+}_{x})^n_j = u'(P_-) \qquad (\nu = 0) \tag{3.20}$$

where u^n_j is defined by Eq. (2.7). By using Eqs. (3.10), (3.11), (3.13), (3.19) and (3.20), one has

$$(\hat{u}^{+}_{x+})^n_j = (\hat{u}^{+}_{x-})^n_j = (\hat{u}^{+}_{x})^n_j = (u^{a+}_{x})^n_j \qquad (\nu = 0) \tag{3.21}$$

Combining Eqs. (3.14) and (3.21), one has

$$(\hat{u}^{w+}_{x})^n_j = (u^{a+}_{x})^n_j \qquad (\nu = 0) \tag{3.22}$$

Thus Eq. (3.15) reduces to Eq. (2.8), i.e., Scheme I reduces to the nondissipative a scheme, in the limit of $\nu \to 0$. QED.

Note that Scheme I can be easily extended to become a 1D Euler solver [3]. However, for an Euler solver, the local *CFL* number must be evaluated in terms of the local flow variables. How it is evaluated will determined the final form of this solver. In the Euler extension of Scheme I (and also Scheme II to be defined later) used by the author, the Euler version of u^n_j, (i.e., $(u_m)^n_j$, $m = 1, 2, 3$, that appear in [3]), is evaluated using the Euler version of Eq. (2.7) (i.e., Eq. (4.24) in [3]). The *CFL* number is then evaluated in terms of $(u_m)^n_j$, $m = 1, 2, 3$. The *CFL* number thus obtained is used in the Euler extensions of Eqs. (3.3)–(3.6) and (3.9)–(3.11).

The Euler version of Scheme I has been extensively evaluated using Sod's shock tube problem. By using a fixed value of α, say $\alpha = 2$, It has been shown that this Euler solver performs much better than the Euler a-α scheme [3] when the global *CFL* number (i.e., the maximal value of local *CFL* numbers) becomes small. Specifically, the new Euler solver can resolve the shock and the contact discontinuity crisply for the global *CFL* number ranging from 1 to less than 0.001. However, in front of the shock, a notable overshoot can appear in the solution generated by the new solver. This overshoot generally can be reduced only by using a larger value of α. To overcome this ad hoc nature of Scheme I, in the following, another solver of Eq. (2.1), referred to as Scheme II, will be constructed through a minor modification of Scheme I.

To proceed, let

$$(s_\pm)^n_j \stackrel{\text{def}}{=} \frac{|(\hat{u}^{+}_{x\pm})^n_j|}{\min(|(\hat{u}^{+}_{x+})^n_j|, |(\hat{u}^{+}_{x-})^n_j|)} - 1 \geq 0 \tag{3.23}$$

Note that, to avoid dividing by zero, in practice a small positive number such as 10^{-60} should be added to the denominator in Eq. (3.23). Using Eqs. (3.12) and (3.23), it can be shown that

$$(\hat{u}^{w+}_{x})^n_j = \frac{[1 + (s_-)^n_j]^\alpha (\hat{u}^{+}_{x+})^n_j + [1 + (s_+)^n_j]^\alpha (\hat{u}^{+}_{x-})^n_j}{[1 + (s_-)^n_j]^\alpha + [1 + (s_+)^n_j]^\alpha} \tag{3.24}$$

For the case that $(s_\pm)^n_j \ll 1$, Eq. (3.24) implies that

$$(\hat{u}^{w+}_{x})^n_j \approx \frac{[1 + \alpha \cdot (s_-)^n_j](\hat{u}^{+}_{x+})^n_j + [1 + \alpha \cdot (s_+)^n_j](\hat{u}^{+}_{x-})^n_j}{2 + \alpha[(s_-)^n_j + (s_+)^n_j]} \tag{3.25}$$

By definition, Scheme II is formed by Eq. (2.7) and

$$(u^{+}_{x})^n_j = \frac{[1 + f(|\nu|)(s_-)^n_j](\hat{u}^{+}_{x+})^n_j + [1 + f(|\nu|)(s_+)^n_j](\hat{u}^{+}_{x-})^n_j}{2 + f(|\nu|)[(s_-)^n_j + (s_+)^n_j]} \tag{3.26}$$

where

$$f(|\nu|) \stackrel{\text{def}}{=} 0.5/|\nu| \tag{3.27}$$

Note that: (i) the expression on the right side of Eq. (3.25) will become that of Eq. (3.26) if each symbol α is replaced by $f(|\nu|)$; and (ii) to avoid dividing by zero, a small positive number should be added to the denominator in Eq. (3.27).

To give the reader a concrete idea about the simplicity and robustness of the CE/SE method in general, and the Euler version of Scheme II in particular, the short and self-contained Fortran program of the solver is listed in Appendix.

4. Numerical results

In this section, accuracy of the Euler a-α solver and the Euler version of Scheme II will be evaluated using Sod's shock tube problem. Without exception, the spatial domain is defined by $-0.505 \leq x \leq 0.505$ with $\Delta x = 0.01$. Also a solution generated by the Euler a-α scheme will be referred to as an old CE/SE

solution while that generated using the Euler version of Scheme II referred to as a new CE/SE solution.

The numerical results at $t = 0.2$, including density (ρ), velocity (u) and pressure (p), are presented for four different sizes of time step, i.e., (i) $\Delta t = 4\times10^{-3}$ (Fig. 4); (ii) $\Delta t = 4\times10^{-4}$ (Fig. 5); (iii) $\Delta t = 4\times10^{-5}$ (Fig. 6); and (iv) $\Delta t = 4 \times 10^{-6}$ (Fig. 7). The values of the global *CFL* number for these four cases approximately are 0.88, 0.088, 0.0088 and 0.00088, respectively. Because each marching step advances a time period $\Delta t/2$, it requires 100, 1,000, 10,000 and 100,000 marching steps for cases (i)–(iv), respectively, to advance to $t = 0.2$.

From the results shown, it is clear that the old CE/SE solution deteriorates quickly as the value of global *CFL* number drops below 0.1. In sharp contract, the new solution is still quite accurate even for the worse case (iv). The advantage of the Euler version of Scheme II over the Euler a-α scheme is overwhelming.

5. Conclusions and discussions

Generally speaking, a stable numerical marching for a non-linear problem requires the presence of a sufficient amount of numerical dissipation. However, accuracy of the numerical results, especially for an unsteady problem, will suffer if too much numerical dissipation is present. As such, a careful control of numerical dissipation is a must for an accurate and stable non-linear unsteady numerical simulation. However, a proper control of numerical dissipation is a very difficult task. Although one can increase the numerical dissipation rather easily, it is much harder to reduce it when accuracy consideration requires it.

Each CE/SE solver is an extension of a core non-dissipative scheme. It is this key feature that make it much easier to reduce numerical dissipation in a CE/SE simulation. It is also the key reason behind the successful construction of the Courant number insensitive CE/SE schemes described in this paper.

As will be shown in future papers, the basic concepts used in the current construction also apply in a multidimensional space. They are also applicable to the cases where the use of nonuniform meshes is required.

Appendix

```
c       A Sample Program
      implicit real*8(a-h,o-z)
      dimension q(3,999),qn(3,999),
     * qx(3,999),qxn(3,999),tq(3),
     * qt(3,999), s(3,999), xx(999)
c       nx must be an odd integer.
      nx = 101
      it = 100
      dt = 0.4d-2
      dx = 0.1d-1
      ga = 1.4d0
      rhol = 1.d0
      ul = 0.d0
      pl = 1.d0
      rhor = 0.125d0
      ur = 0.d0
      pr = 0.1d0
      nx1 = nx + 1
      nx2 = nx1/2
      hdt = dt/2.d0
      hdx = dx/2.d0
      tt = hdt*dfloat(it)
      qdt = dt/4.d0
      qdx = dx/4.d0
      dtx = dt/dx
      a1 = ga - 1.d0
      a2 = 3.d0 - ga
      a3 = a2/2.d0
      a4 = 1.5d0*a1
      u2l = rhol*ul
      u3l = pl/a1 + 0.5d0*rhol*ul**2
      u2r = rhor*ur
      u3r = pr/a1 + 0.5d0*rhor*ur**2
      do 5 j = 1,nx2
      q(1,j) = rhol
      q(2,j) = u2l
      q(3,j) = u3l
      q(1,nx2+j) = rhor
      q(2,nx2+j) = u2r
      q(3,nx2+j) = u3r
      do 5 i = 1,3
      qx(i,j) = 0.d0
      qx(i,nx2+j) = 0.d0
    5 continue
      open (unit=8,file='for008')
      do 400 i = 1,it
      m = nx + i - (i/2)*2
      do 100 j = 1,m
      w2 = q(2,j)/q(1,j)
      w3 = q(3,j)/q(1,j)
      f21 = -a3*w2**2
      f22 = a2*w2
      f31 = a1*w2**3 - ga*w2*w3
      f32 = ga*w3 - a4*w2**2
      f33 = ga*w2
      qt(1,j)=-qx(2,j)
      qt(2,j)=-(f21*qx(1,j)+f22*qx(2,j)+a1*qx(3,j))
      qt(3,j)=-(f31*qx(1,j)+f32*qx(2,j)+f33*qx(3,j))
      s(1,j)=qdx*qx(1,j)+dtx*(q(2,j)+qdt*qt(2,j))
      s(2,j)=qdx*qx(2,j)+dtx*(f21*(q(1,j)+
     * qdt*qt(1,j))+f22*(q(2,j)+qdt*qt(2,j))+
     * a1*(q(3,j)+qdt*qt(3,j)))
```

```
  s(3,j)=qdx*qx(3,j)+dtx*(f31*(q(1,j)+
  * qdt*qt(1,j))+f32*(q(2,j)+qdt*qt(2,j))+
  * f33*(q(3,j)+qdt*qt(3,j)))
100 continue
  if (i.ne.(i/2)*2) goto 150
  do 120 k = 1,3
  qx(k,nx1) = qx(k,nx)
  qn(k,1) = q(k,1)
  qn(k,nx1) = q(k,nx)
120 continue
150 j1 = 1 - i + (i/2)*2
  mm = m - 1
  do 200 j = 1,mm
  do 180 k = 1,3
  tq(k)=0.5d0*(q(k,j)+q(k,j+1)+s(k,j)-
  * s(k,j+1))
180 continue
  x = dabs(tq(2)/tq(1))
  y = a1*(tq(3) - 0.5d0*x**2*tq(1))
  c = dsqrt(ga*y/tq(1))
  cn = (dtx*(c+x))
  dx1 = (1.d0 + cn)*qdx
  dx2 = hdx - dx1
  do 200 k = 1,3
  vxl=(tq(k)-q(k,j)-dx2*qx(k,j)-hdt*qt(k,j))/dx1
  vxr=(q(k,j+1)+hdt*qt(k,j+1)-dx2*qx(k,j+1)-
  * tq(k))/dx1
  rz = dmin1(dabs(vxl),dabs(vxr)) + 1.d-60
  sl = dabs(vxl)/rz - 1.d0
  sr = dabs(vxr)/rz - 1.d0
  alp = 0.5d0/(cn + 1.d-60)
  qxn(k,j+j1) = (vxl*(1.d0 + alp*sr) + vxr*
  * (1.d0 + alp*sl))/(2.d0 + alp*(sr + sl))
  qn(k,j+j1) = tq(k)
200 continue
  m = nx1 - i + (i/2)*2
  do 300 j = 1,m
  do 300 k = 1,3
  q(k,j) = qn(k,j)
  qx(k,j) = qxn(k,j)
300 continue
400 continue
  m = nx1 -it + (it/2)*2
  mm = m - 1
  xx(1) = -0.5d0*dx*dfloat(mm)
  do 500 j = 1,mm
  xx(j+1) = xx(j) + dx
500 continue
  do 600 j = 1,m
  x = q(2,j)/q(1,j)
  y = a1*(q(3,j) - 0.5d0*x**2*q(1,j))
  z = x/dsqrt(ga*y/q(1,j))
  write (8,50) xx(j),q(1,j),x,y,z
600 continue
  close (unit=8)
50 format(' x =',f8.4,' rho =',f8.4,' u =',f8.4,
  * ' p =',f8.4,' M =',f8.4)
  stop
  end
```

References

1. S.C. Chang and W.M. To, *A New Numerical Framework for Solving Conservation Laws–The Method of Space-Time Conservation Element and Solution Element*, NASA TM 104495, August 1991.

2. S.C. Chang and W.M. To, A brief description of a new numerical framework for solving conservation laws—The method of space-time conservation element and solution element, in *Proceedings of the Thirteenth International Conference on Numerical Methods in Fluid Dynamics, Rome, Italy, 1992*, edited by M. Napolitano and F. Sabetta, Lecture Notes in Physics 414, (Springer-Verlag, New York/Berlin, 1992), p. 396.

3. S.C. Chang, The method of space-time conservation element and solution Element—A new approach for solving the Navier-Stokes and Euler equations, *J. Comput. Phys.*, **119**, 295 (1995).

4. S.C. Chang, S.T. Yu, A. Himansu, X.Y. Wang, C.Y. Chow, and C.Y. Loh, The method of space-time conservation element and solution element—A new paradigm for numerical solution of conservation laws, in *Computational Fluid Dynamics Review 1998* edited by M.M. Hafez and K. Oshima (World Scientific, Singapore), Vol. 1, p. 206.

5. T. Molls and F. Molls, "Space-Time Conservation Method Applied to Saint Venant Equations," *J. of Hydraulic Engr.*, **124(5)**, 501 (1998).

6. C. Zoppou and S. Roberts, "Space-Time Conservation Method Applied to Saint Venant Equations: A Discussion," *J. of Hydraulic Engr.*, **125(8)**, 891 (1999).

7. S.C. Chang, X.Y. Wang, and C.Y. Chow, The space-time conservation element and solution element method: A new high-resolution and genuinely multidimensional paradigm for solving conservation laws," *J. Comput. Phys.*, **156**, 89 (1999).

8. X.Y. Wang, and S.C. Chang, A 2D non-splitting unstructured triangular mesh Euler solver based on the space-time conservation element and solution element method, *Computational Fluid Dynamics Journal*, **8(2)**, 309 (1999).

9. S.C. Chang, X.Y. Wang and W.M. To, Application of the space-time conservation element and solution element method to one-dimensional convection-diffusion problems, *J. Comput. Phys.*, **165**, 189 (2000).

10. J. Qin, S.T. Yu, Z.C. Zhang, and M.C. Lai, Direct Calculations of Cavitating Flows by the Space-Time CE/SE Method, *J. Fuels & Lubricants, SAE Transc.*, **108(4)**, 1720 (2000).

11. C.Y. Loh, L.S. Hultgren and S.C. Chang, Wave computation in compressible flow using the space-time conservation element and solution element method, *AIAA J.*, **39(5)**, 794 (2001).

12. Z.C. Zhang, S.T. Yu, and S.C. Chang, A Space-Time Conservation Element and Solution Element Method for Solving the Two- and Three-Dimensional Unsteady Euler Equations Using Quadrilateral and Hexahedral Meshes, *J. Comput. Phys.*, **175**, 168 (2002).

13. K.B.M.Q. Zaman, M.D. Dahl, T.J. Bencic, and C.Y. Loh, Investigation of A 'Transonic Resonance' with Convergent-Divergent Nozzles, accepted for publication in *Journal of Fluid Mechanics*.

14. C.Y. Loh and K.B.M.Q. Zaman, *Numerical Investigation of 'Transonic Resonance' with A Convergent-Divergent Nozzle*, AIAA Paper 2002-0077, also accepted for publication in *AIAA J.*.

15. X.Y. Wang, C.Y. Chow, and S.C.Chang, *Numerical Simulation of Flows Caused by Shock-Body Interaction*, AIAA Paper 96-2004 (1996).

16. S.C. Chang, A. Himansu, C.Y. Loh, X.Y., Wang, S.T., Yu, and P. Jorgenson, Robust and Simple Non-Reflecting Boundary Conditions for the Space-Time Conservation Element and Solution Element Method, in *A Collection of Technical Papers, 13th AIAA CFD Conference, June 29-July 2, 1997, Snowmass, Colorado*, AIAA Paper 97-2077.

17. C.Y. Loh, L.S. Hultgren and S.C. Chang, *Vortex Dynamics Simulation in Aeroacoustics by the Space-Time Conservation Element and Solution Element Method*, AIAA Paper 99-0359 (1999)

18. X.Y. Wang, S.C. Chang and P.C.E. Jorgenson, *Accuracy Study of the Space-Time CE/SE Method for Computational Aeroacoustics Problems Involving Shock Waves*, AIAA Paper 2000-0474 (2000).

19. C.Y. Loh, L.S. Hultgren, S.C. Chang and P.C.E. Jorgenson, *Noise Computation of a Supersonic Shock-Containing Axisymmetric Jet by the CE/SE Method*, AIAA Paper 2000-0475 (2000).

20. C.Y. Loh, X.Y. Wang, S.C. Chang, and P.C.E. Jorgenson, Computation of Feedback Aeroacoustic System by the CE/SE Method, in *Proceedings of the First International Conference on Computational Fluid Dynamics, Kyoto, Japan, 10-14 July, 2000*, edited by N. Satofuka, (Springer-Verlag Berlin Heiderberg 2001), p. 555.

21. C.Y. Loh, L.S. Hultgren and P.C.E. Jorgenson, *Near Field Screech Noise Computation for An Underexpanded Supersonic Jet by the CE/SE Method*, AIAA Paper 2001-2252 (2001).

22. X.Y. Wang, S.C. Chang, and P.C.E. Jorgenson, Numerical Simulation of Aeroacoustic Field in a 2D Cascade Involving a Downstream Moving Grid Using the Space-Time CE/SE method, in *Proceedings of the First International Conference on Computational Fluid Dynamics, Kyoto, Japan, 10-14 July, 2000*, edited by N. Satofuka, (Springer-Verlag Berlin Heiderberg 2001), p. 543.

23. X.Y. Wang, S.C. Chang, A. Himansu, and P.C.E. Jorgenson, *Gust Acoustic Response of A Single Airfoil Using the Space-Time CE/SE Method*, AIAA Paper 2002-0801 (2002).

24. S.T. Yu and S.C. Chang, *Treatments of Stiff Source Terms in Conservation Laws by the Method of Space-Time Conservation Element and Solution Element*, AIAA Paper 97-0435 (1997).

25. S.T. Yu and S.C. Chang, Applications of the Space-Time Conservation Element / Solution Element Method to Unsteady Chemically Reactive Flows," AIAA Paper 97-2099, in *A Collection of Technical Papers, 13th AIAA CFD Conference*, June 29-July 2, 1997, Snowmass, CO.

26. S.T. Yu, S.C. Chang, P.C.E. Jorgenson, S.J. Park and M.C. Lai, "Treating Stiff Source Terms in Conservation Laws by the Space-Time Conservation Element and Solution Element Method," in *Proceedings of the 16th International Conference on Numerical Method in Fluid Dynamics, Arcachon, France, 6-10 July, 1998*, edited by C.H. Bruneau, (Springer-Verlag Berlin Heidelberg 1998), p. 433.

27. X.Y. Wang and S.C. Chang, A 3D structured/unstructured Euler solver based on the space-time conservation element and solution element method, in *A Collection of Technical Papers, 14th AIAA CFD Conference, June 28–July 1, 1999, Norfolk, Virginia*, AIAA Paper 99-3278.

28. N.S. Liu and K.H. Chen, *Flux: An Alternative Flow Solver for the National Combustion Code*, AIAA Paper 99-1079.

29. G. Cook, *High Accuracy Capture of Curved Shock Front Using the Method of Conservation Element and Solution Element*, AIAA Paper 99-1008.

30. S.C. Chang, Y. Wu, X.Y. Wang, and V. Yang, Local Mesh Refinement in the Space-Time CE/SE Method, in *Proceedings of the First International Conference on Computational Fluid Dynamics, Kyoto, Japan, 10-14 July, 2000*, edited by N. Satofuka, (Springer-Verlag Berlin Heiderberg 2001), p. 61.

31. S.C. Chang, Z.C. Zhang, S.T. John Yu, and P.C.E. Jorgenson, A Unified Wall Boundary Treatment for Viscous and Inviscid Flows in the CE/SE Method, in *Proceedings of the First International Conference on Computational Fluid Dynamics, Kyoto, Japan, 10-14 July, 2000*, edited by N. Satofuka, (Springer-Verlag Berlin Heiderberg 2001), p. 671.

32. Z.C. Zhang, S.T. John Yu, S.C. Chang, and P.C.E. Jorgenson, Calculations of Low-Mach-Number Viscous Flows without Preconditioning by the Space-Time CE/SE method, in *Proceedings of the First International Conference on Computational Fluid Dynamics, Kyoto, Japan, 10-14 July, 2000*, edited by N. Satofuka, (Springer-Verlag Berlin Heiderberg 2001), p. 127.

33. A. Himansu, P.C.E. Jorgenson, X.Y. Wang, and S.C. Chang, Parallel CE/SE Computational via Domain Decomposition, in *Proceedings of the First International Conference on Computational Fluid Dynamics, Kyoto, Japan, 10-14 July, 2000*, edited by N. Satofuka, (Springer-Verlag Berlin Heiderberg 2001), p. 423.

34. Y. Wu, V. Yang, and S.C. Chang, Space-Time Method for Chemically Reacting Flows with Detailed Kinetics, in *Proceedings of the First International Conference on Computational Fluid Dynamics, Kyoto, Japan, 10-14 July, 2000*, edited by N. Satofuka, (Springer-Verlag Berlin Heiderberg 2001), p. 207.

35. Other CE/SE references are posted on: (i) http://www.grc.nasa.gov/www/microbus, and (ii) http://www.cfd.eng.wayne.edu.

36. G.A. Sod, A Survey of several Finite Difference Methods for Systems of Nonlinear Hyperbolic Conservation Laws, *J. Comput. Phys.*, **27**, 1 (1978).

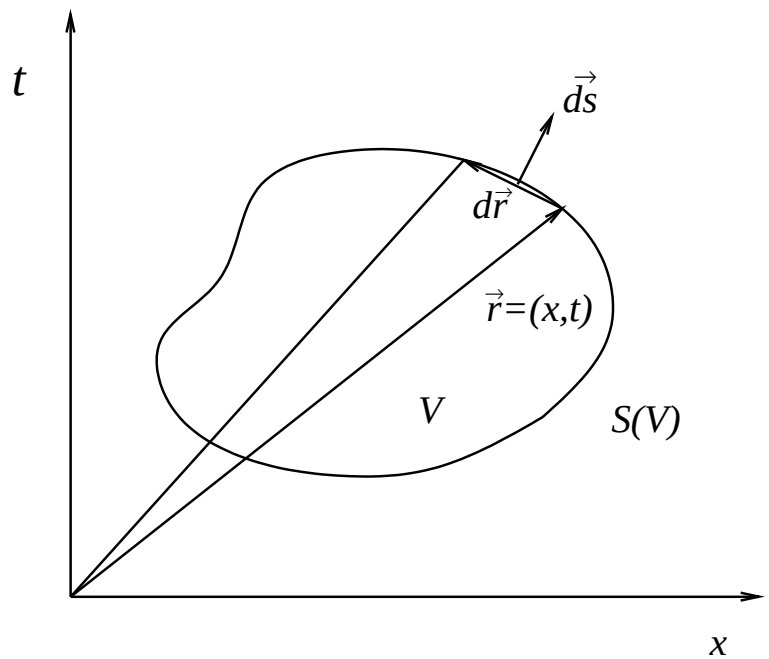

Figure 1. — A surface element on the boundary S(V) of an arbitrary space-time volume V.

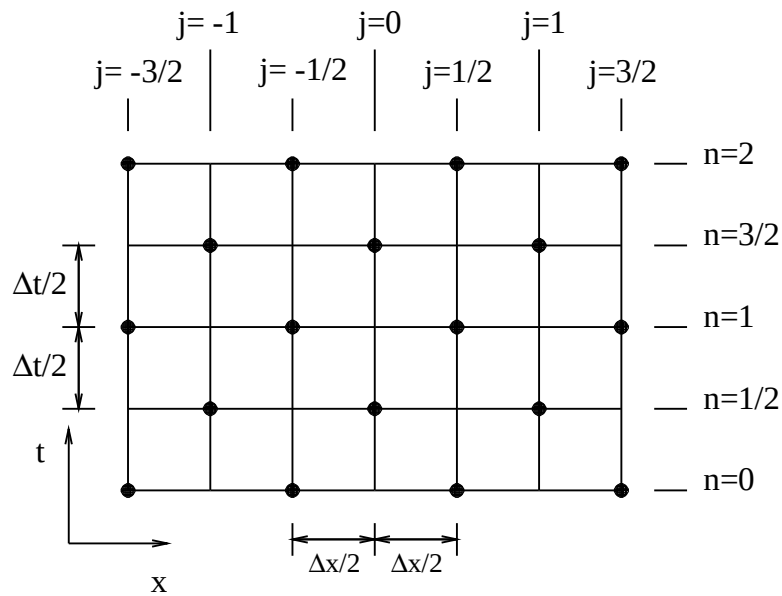

2(a). — The space-time mesh.

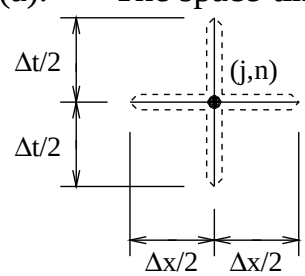

2(b). — SE(j,n)

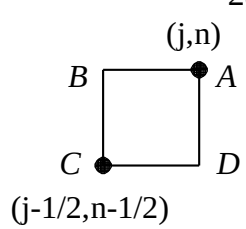

2(c). $CE_-(j,n)$

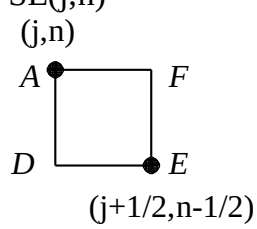

2(d). $CE_+(j,n)$

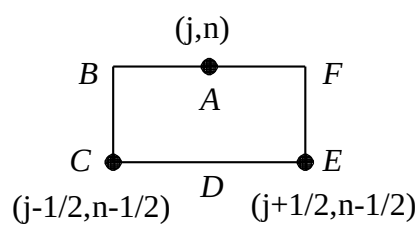

2(e). CE(j,n)

Figure 2. — The SEs and CEs.

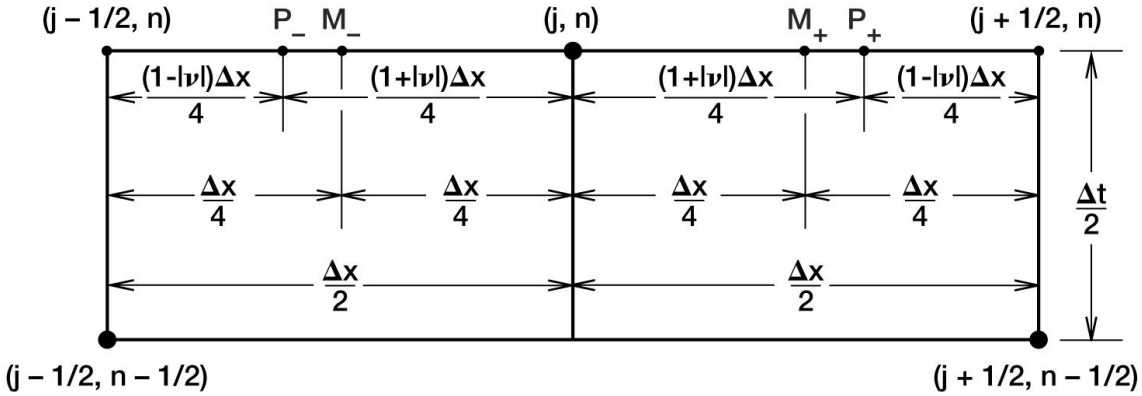

Figure 3.—Definition of points P_-, M_-, M_+ and P_+.

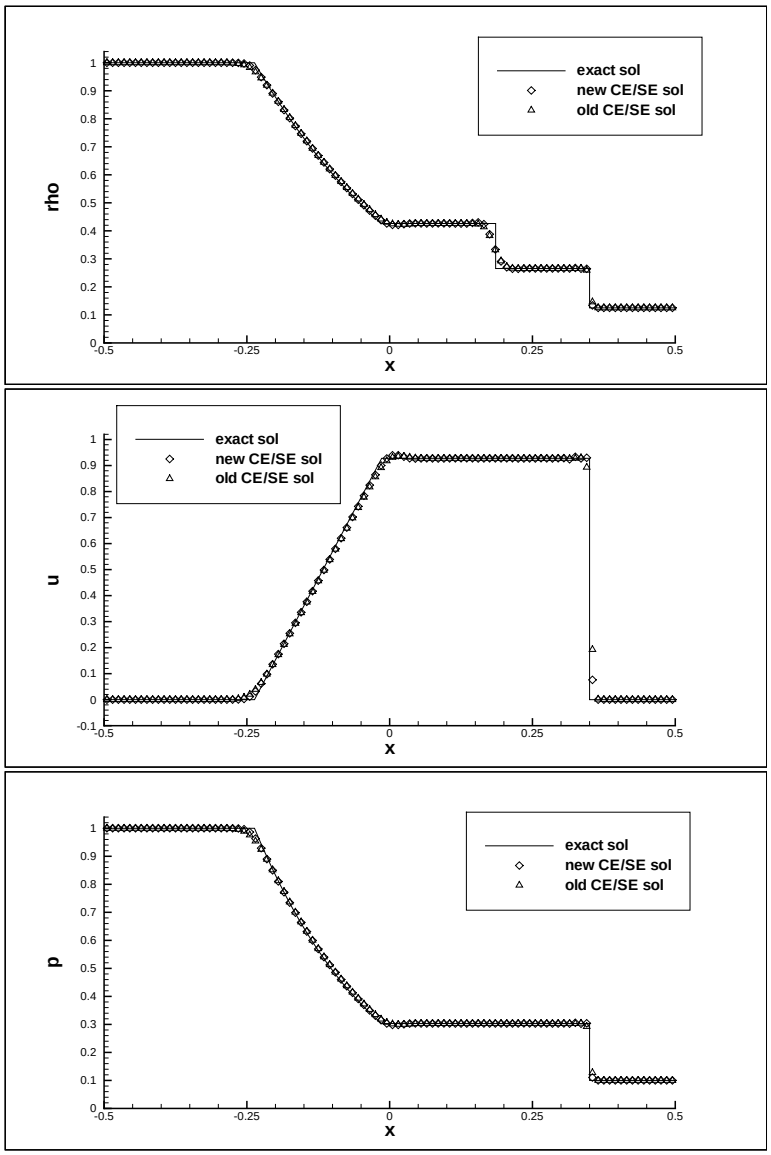

Figure 4: Solution comparison at $CFL = 0.88$.

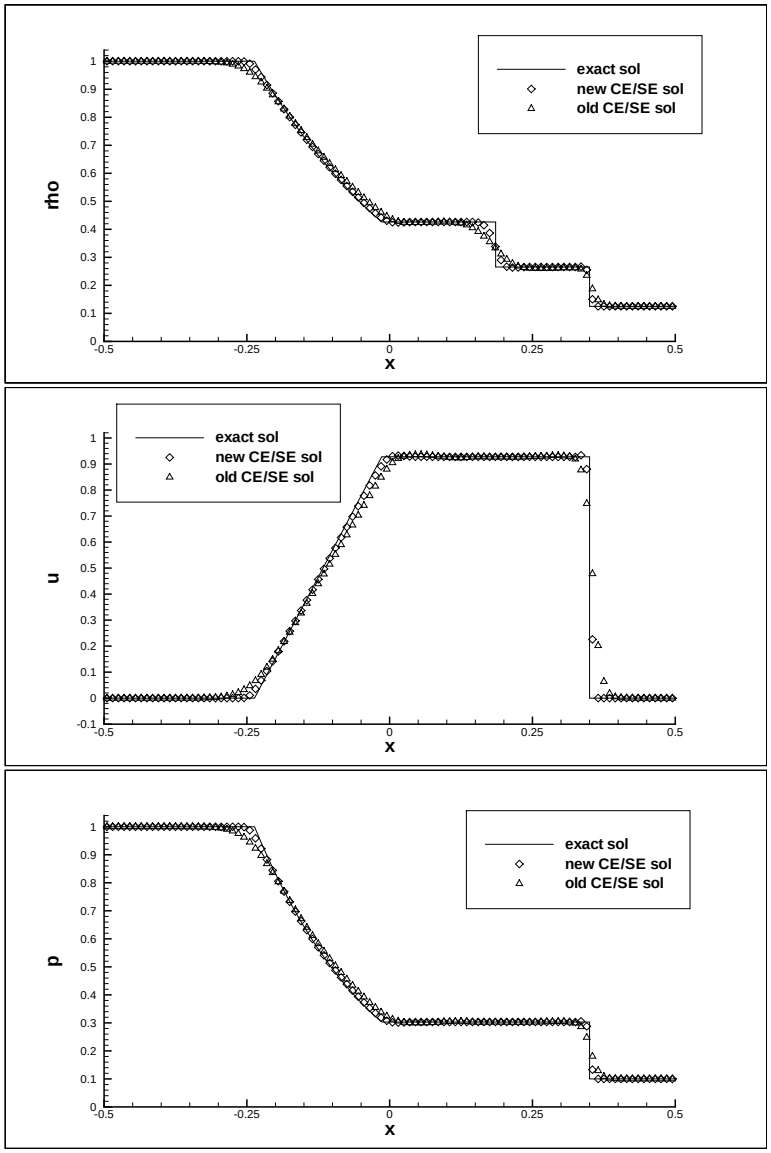

Figure 5: Solution comparison at $CFL = 0.088$.

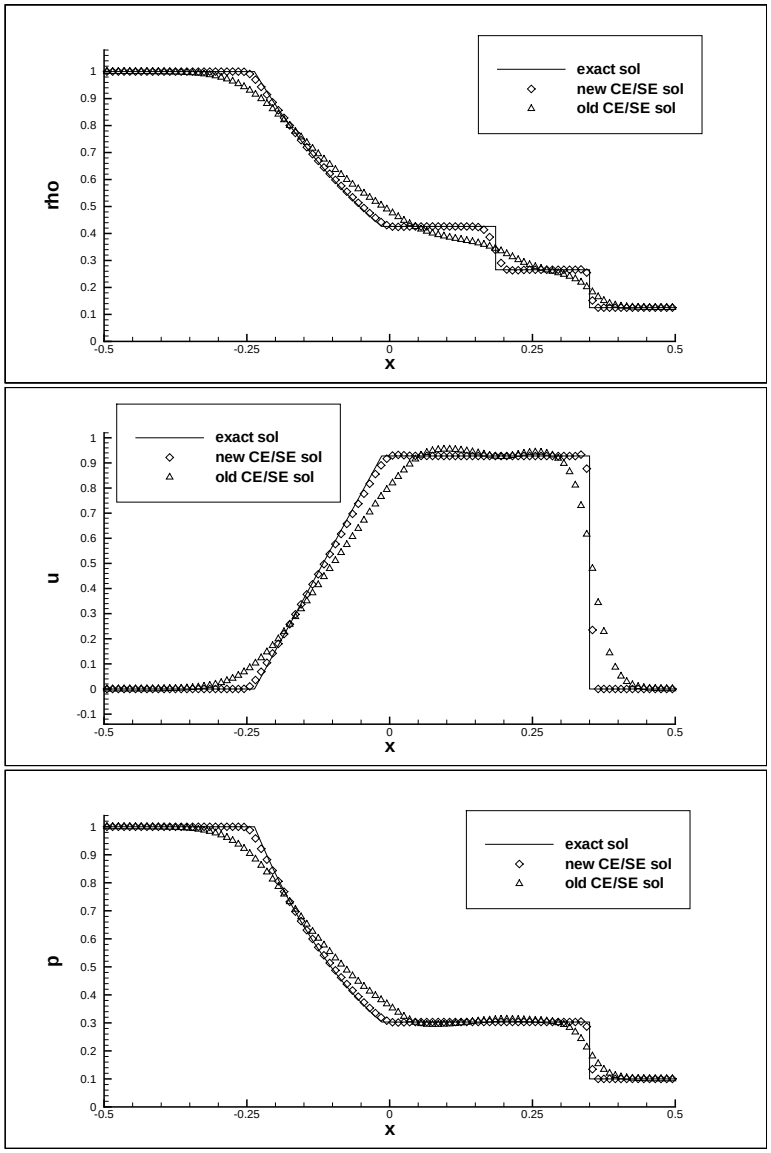

Figure 6: Solution comparison at $CFL = 0.0088$.

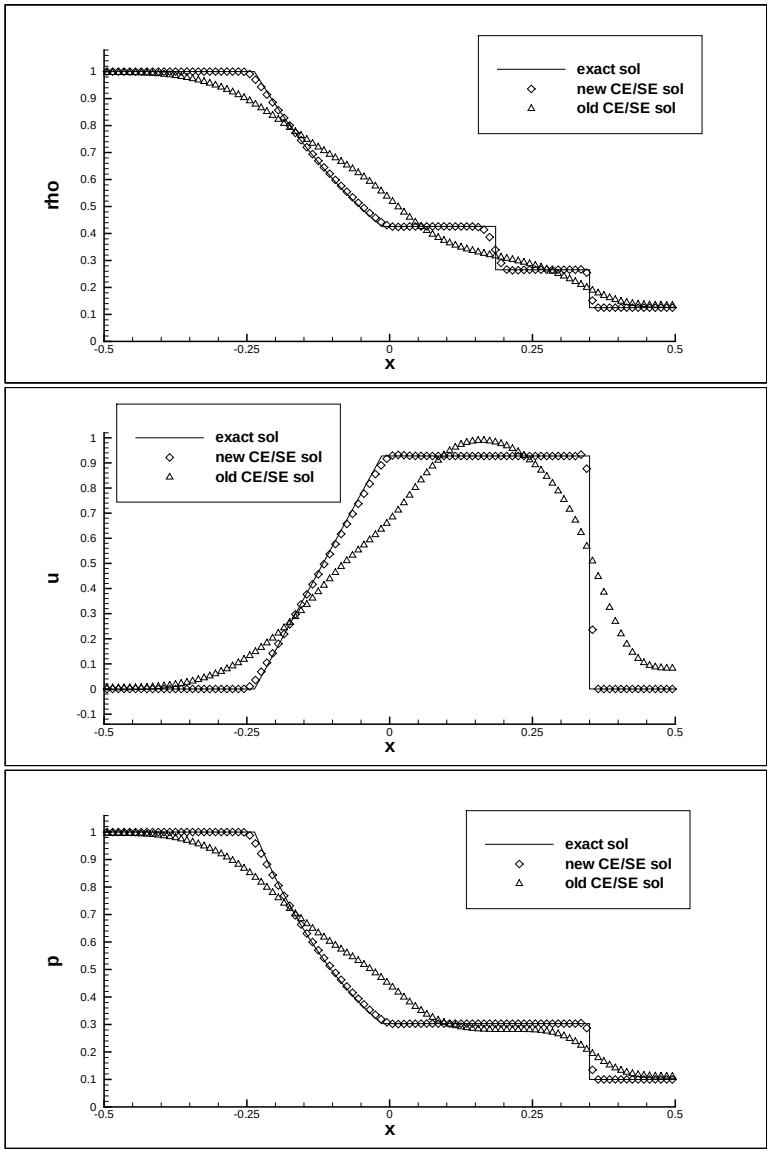

Figure 7: Solution comparison at $CFL = 0.00088$.